

## Neutron Production in Ag, Ta, Au, Pt, and Pb by the Interaction of 7.5–14-MeV Protons\*

RICHARD G. THOMAS, JR., AND W. BARTOLINI

*Lawrence Radiation Laboratory, University of California, Livermore, California*

(Received 25 July 1966; revised manuscript received 19 January 1967)

Use was made of a large liquid scintillator to determine excitation functions for  $(p,n)$  and  $(p,2n)$  interactions in Ag, Ta, Au, Pt, and Pb. A value of 1.6 F was deduced for  $r_0$ , the nuclear radius parameter. Comparison of these data with the reaction cross sections obtained in another experiment confirms that neutron production is the dominant process for these elements at 10 MeV. The simple statistical model in which only neutron emission is assumed provides a reasonably satisfactory explanation of the observed behavior, but other results indicate that the  $(p,pn)$  process could be significant in these elements.

### INTRODUCTION

OVER the years considerable information has been obtained on the production of neutrons by the interaction of charged particles with various nuclei. A few of the many experiments are listed below.<sup>1-4</sup> Experimenters have usually employed the methods of foil activation and of direct neutron counting. The former technique requires a relatively small amount of experimental equipment, but is limited to those isotopes whose decay rates and schemes are known and measurable. An advantage of this limitation is that one can frequently use foils with their normal mixture of isotopes to extract the neutron production cross sections of specific isotopes. Direct neutron counting requires no knowledge of decay rates and schemes, but in general involves a more elaborate experimental setup. Moreover, this technique does not allow one to separate the effects of individual isotopes when one uses foils containing a mixture of them. The experiment described here involved counting neutrons produced in foils of natural isotopic composition. For those elements that are not mono-isotopic, our results therefore are averages over the various isotopes.

The elements studied and the energies employed are such that one expects the continuum theory to describe adequately the observed phenomena. Therefore, we compared our results with predictions given by this theory.

This experiment is an extension and expansion of work previously reported.<sup>5</sup> After the introduction of several techniques designed to test the consistency and increase the reliability of the results, we repeated the measurements on Ag, Ta, and Au. This report contains our most recent data on these elements and on the elements Pt and Pb which were not studied earlier.

\* This work was performed under the auspices of the U. S. Atomic Energy Commission.

<sup>1</sup> H. Taketani and W. P. Alford, *Phys. Rev.* **125**, 291 (1962).

<sup>2</sup> S. Tanaka and M. Furukawa, *J. Phys. Soc. Japan* **14**, 1260 (1959).

<sup>3</sup> J. W. Meadows, *Phys. Rev.* **91**, 885 (1953).

<sup>4</sup> B. Linder and R. James, *Phys. Rev.* **114**, 322 (1959).

<sup>5</sup> G. Chodil, R. C. Jopson, H. Mark, C. D. Swift, R. G. Thomas, and M. K. Yates, *Nucl. Phys.* **A93**, 648 (1967).

### NEUTRON DETECTION

The neutrons were detected by use of a large liquid scintillator. This tank was described previously,<sup>6</sup> but has since been modified. The main modifications were the increase in the inner diameter from 6 to 12 in., and a decrease in the length from 40 to 33 in. The diameter was increased to accommodate a foil-changing mechanism that allowed six different targets to be selected. The length was decreased to allow additional shielding at the rear. These geometrical changes reduced the tank volume from 240 to 170 gal. In accordance with the new dimensions, the number of photomultiplier tubes (DuMont 6364) mounted over the outside surface was decreased from 24 to 16.

The tank was filled with toluene that contained 10 g/liter gadolinium ocoate, 5 g/liter *p*-terphenyl, and 0.1 g/liter POPOP [2, 2'-*p*-phenylene-bis-(5-phenyl-oxazole)]. The inside surface was covered with white paint which has a high reflectivity in the visible region.<sup>7</sup> The detection process consisted of moderating the incoming neutrons by collisions with hydrogen, followed by capture in hydrogen or gadolinium. The high capture cross section of the latter and the amount used ensured that about 25 neutrons were captured in gadolinium for every one that was captured by hydrogen. An average of three of four  $\gamma$  rays result from capture in gadolinium. This accounts for the high efficiency of this device as a neutron detector.

### ELECTRONICS AND CURRENT MEASUREMENT

The beam geometry that was employed at the Livermore 90-in. cyclotron is shown in Fig. 1.

A block diagram of the electronics is shown in Fig. 2. A pulsed beam, operating at a frequency of about 2 kc/sec, passed through the target which was located at the center of the 1-ft-diam through-tube that served as the inner surface of the tank. The pulser was triggered by the cyclotron rf system. The beam then passed through a  $\frac{1}{2}$ -in.-thick parallel plate ion chamber which

<sup>6</sup> V. J. Ashby, H. C. Catron, L. L. Newkirk, and C. J. Taylor, *Phys. Rev.* **111**, 616 (1958).

<sup>7</sup> Supplied by Wisconsin Protective Coating Company.

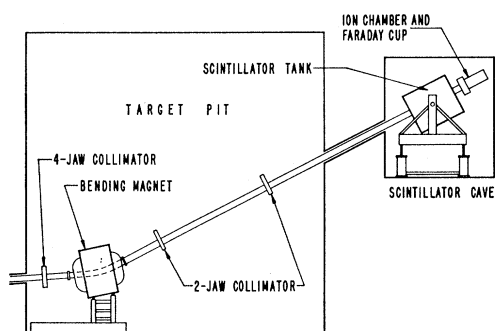


Fig. 1. Experimental geometry.

served to monitor its intensity, and was then stopped in an 8-in.-diam Faraday cup. This chamber was located about 2 ft behind the tank and contained He gas at  $\frac{1}{6}$ -atm pressure. The gas was confined by two thin Al foils of 1-mil thickness.

Figure 3 shows the probability per unit time of observing neutron captures in the scintillator at a time  $t$  after passage of the beam through the target. The passage of the beam through the target was evidenced by the appearance of prompt  $\gamma$  rays. Neutrons entered the tank at about time zero, were moderated shortly thereafter, and were then captured over an interval of about 50  $\mu$ sec. It is readily deducible from the graph that 95% of the captures take place during this interval. The counting system shown in Fig. 2 was gated on about 1  $\mu$ sec following the appearance of the prompt  $\gamma$ 's. Coincidence pulses received by one or more tubes in each of the two banks were stored in the memory until after the counting interval ended. The total number received during that burst beam pulse was then recorded in one of the nine scalars that record multiplicities from 0 to 8. The intensity of the beam was adjusted so that it was unlikely that more than eight coincidence pulses per burst were present. Usually no more than six or seven pulses per burst were recorded.

The analysis of the data was made under the assumption that the burst intensity was constant. There

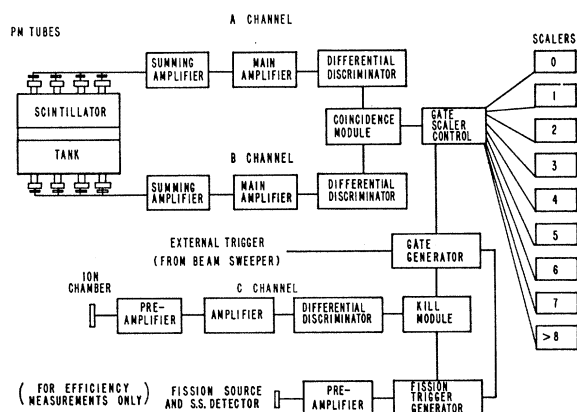


Fig. 2. Block diagram of electronics.

was, however, wide fluctuation in cyclotron burst intensities, and therefore not all were acceptable. The selection of bursts of uniform intensity was made with the ion chamber and a circuit designated "kill" designed for this purpose. For a fixed proton beam energy, the pulse height from the chamber was proportional to the burst intensity. A discriminator allowed only pulses that fell within the adjustable "kill" window to be accepted. A typical run consisted of  $5 \times 10^4$  accepted pulses. At the end of the run there was a distribution of counts  $n_i$  among the  $i$  scalars such that

$$\sum_{i=0}^8 n_i = 5 \times 10^4.$$

The total number of events, represented by

$$\sum_{i=1}^8 i n_i,$$

was determined by the average current during the run. When the discriminator window was too wide, a repeti-

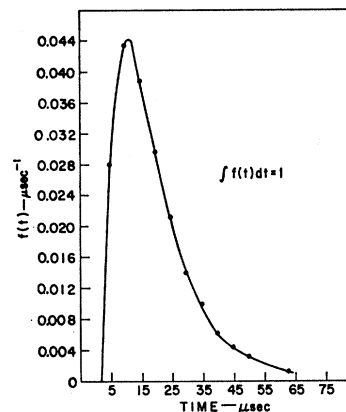


Fig. 3. Normalized neutron capture-time spectrum.

tion of the run produced both a different distribution of events among the scalars and a different number of total events. This was because the beam pulse distribution was time-dependent and the average current was not, in general, the same in the two cases. For a sufficiently narrow window however, the same distribution of events (within statistical limitations) was obtained repeatedly, and this condition was used to determine the maximum width of the window. A value that included approximately 5% of the beam bursts was generally found to be satisfactory. Bursts that were not accepted caused the "kill" circuit to erase the contents of the memory unit instead of recording them.

The intensity of the accepted bursts was deduced by correlating for a fixed number of them, the total number of neutrons obtained from a target with and without the "kill" circuit connected. With the "kill" circuit inoperative, the total number of neutrons was determined as a function of the integrated charge. This relationship was found to be linear. With the "kill" circuit

operating, the total number of neutrons was again determined, for the same number of beam bursts. The beam intensity was then inferred.

The energy of the beam was determined by the standard technique of elastically scattering a portion of the beam into aluminum absorbers, and measuring the range of the scattered particles. The error in this technique was about 1% and was due primarily to the inaccuracy of the range-energy relations for protons in Al. As a check on this method, we also allowed the beam particles to scatter elastically off a foil of Au into a solid-state detector where they were stopped. This device was calibrated by using the known energies of two  $\alpha$  sources. The difference between the energies, as determined by the two methods was always less than  $\pm 0.2$  MeV.

### DETECTOR EFFICIENCY

Needed in the analysis was the efficiency of neutron detection. This quantity was determined by a  $\text{Cf}^{252}$  fission source mounted in front of a solid-state detector. The combination was then placed in the center of the tank. Pulses from fission fragments were fed into a secondary fission trigger generator that activated the neutron counter (see Fig. 2). Included in this secondary trigger generator is a feature that causes the "kill" circuit to erase the memory contents if two fissions occur during the counting interval. Referring to the work of Diven *et al.*<sup>8</sup> for  $\bar{\nu}$ , the average number of neutrons per fission, we calculated an efficiency of  $(62 \pm 2)\%$ . As a check on this value, a second method was used to determine the tank efficiency. For this method, a Pu-Be source and a 2-in.  $\times$  2-in. NaI(Tl) crystal were mounted at the center of the tank. The counter in this case was triggered by pulses resulting from the 4.43-MeV excited state in  $\text{C}^{12}$ . Within the error quoted above, agreement was obtained between the two methods. This agreement also demonstrated the insensitivity of the system to the change in neutron spectrum.

### DATA ANALYSIS

Initially, the data were handled in a manner similar to that previously described.<sup>6</sup> The probability per burst counting  $m$  real events in the scintillator was calculated from the equation

$$P_m = [F_m - \sum_{n=1}^m P_{m-n} B_n] \frac{1}{B_0}. \quad (1)$$

In Eq. (1)  $F_m$  is the probability per burst of getting  $m$  events, real and background, while  $B_n$  is the probability of getting  $n$  background events. The quantity  $P_m$  was next corrected for losses due to time resolution. This

correction was approximately 2%. The probability per burst  $s(n)$ , of making  $n$  neutrons in a foil is given by

$$s(n) = \sum_{m=n}^8 A_{m,n} P_m^c, \quad (2)$$

where  $P_m^c$  is the corrected value of  $P_m$ , and

$$A_{m,n} = \frac{m! E^{-m}}{n!(m-n)!} (1-E)^{m-n} (-1)^{m-n}. \quad (3)$$

$E$  is the chamber efficiency. The average number  $\bar{x}$  of  $(p,n)$  and  $\bar{y}$  of  $(p,2n)$  interactions per burst was obtained by comparing  $s(n)$  with  $f(n)$ , the Poisson expression for making  $n$  neutrons using all possible combinations of  $(p,n)$  and  $(p,2n)$  reactions. These expressions are

$$\begin{aligned} f_0 &= \exp[-(\bar{x} + \bar{y})], \\ f_1 &= \bar{x} f_0, \\ f_2 &= (\frac{1}{2}\bar{x}^2 + \bar{y}) f_0, \\ &\text{etc.} \end{aligned} \quad (4)$$

A least-squares procedure was used to minimize

$$R = \sum_{n=0}^8 w(n) [s(n) - f(n)]^2 \quad (5)$$

with respect to  $\bar{x}$  and  $\bar{y}$ . Because of intensity limitations, only the first three to five values of  $n$  were significant. The weight  $w(n)$  of each significant value was arbitrarily set equal to 1.

### DISCUSSION OF ERRORS

Statistical errors amounted to no more than  $\pm 3\%$ , and in most cases were considerably less. The chamber efficiency has been found to hold steady within 4% over a period of months. Most of the foils were obtained from Oak Ridge, though a few were obtained at this laboratory. Impurities, as estimated by the supplier, were usually less than 0.1% and were considered negligible. A check of foil uniformity with an  $\alpha$  source resulted in the assignment of an error of 5% to the quoted thicknesses. The quantity that presents the greatest potential for systematic error was the current because of its magnitude and because of multiple scattering. Its value was of the order of  $10^{-11}$  A. To determine the charge associated with this small current, we allowed the recorder output of a picoammeter to drive a conventional beam current integrator. The system was calibrated by use of a constant-current dc source. The accuracy of this procedure was checked by simultaneously counting the beam particles scattered from a foil of Au and integrating the charge passing through the foil. Using the Coulomb scattering law, we calculated the current and compared it with that directly read. Differences averaging 10% were obtained. These could be ascribed, however, to the finite dimensions of the

<sup>8</sup> B. C. Diven, H. C. Martin, R. F. Taschek, and J. Tenell, Phys. Rev. **101**, 1012 (1956).

beam, and to the uncertainty in the solid angle at the detector. The soundness of this technique for measuring charge was thus considered demonstrated by this agreement. The effect of multiple scattering was investigated by calculating the quantity  $(\sigma_n + 2\sigma_{2n})$  without the ion chamber in place and comparing with the value obtained when it was used. This quantity is a measure of the total number of neutrons produced, and depends only on the integrated charge. Again differences of about  $\pm 10\%$  were observed. Since the reproducibility of the cross sections was of this order, it was concluded that multiple-scattering corrections were negligible. On the basis of these results, and of the agreement between our  $(p,n)$  cross sections for Ta and those previously measured,<sup>9</sup> we concluded that no correction was needed for systematic error in the current. An uncertainty of  $\pm 5\%$  was assigned to values used to account for all unknown sources of error. A study was made to determine if delayed  $\gamma$ 's were causing too many events to be counted. The foils were surrounded by 1-in.-thick lead cylinders. The length of these cylinders was such that  $\gamma$ 's had to pass through the lead to enter the chamber. Cross sections calculated with and without the surrounding cylinders were the same within  $\pm 10\%$ . Thus, very few delayed  $\gamma$ 's were counted and no correction was made. The quoted errors in cross sections represent the result of propagating the above-mentioned ones through the equations defining them.

## RESULTS AND CONCLUSIONS

The values obtained for the excitation functions, along with the calculated errors, are given in Tables I and II. Since the detector does not distinguish between  $(p,n)$  and  $(p,pn)$ , the results in Table I represent the sum of these two interactions. For comparison we also present the results of Hansen *et al.*,<sup>9</sup> who studied Au and Ta.

TABLE I. Tabulation of observed  $(p,pn) + (p,n)$  cross sections.

Energy (MeV)	Ta <sup>a</sup>	Ta	Au <sup>a</sup>	Cross section (mb)			
				Au	Ag	Pb	Pt
7.6	30	39±9	5.5	32±6	313±15	30±8	30±5
8.1	51	64±9	28	50±10	379±17	51±8	56±5
8.5	75	86±10	40	65±13	450±22	69±10	73±6
9.0	92	108±16	56	78±18	489±24	91±13	93±8
9.7	104	104±15	79	119±20	549±26	140±13	142±8
10.0	104	124±25	90	153±35	573±35	202±27	197±17
10.6	98	99±20	93	133±27	595±29	257±17	221±12
11.1	90	61±30	93	109±50	544±36	306±38	207±23
11.5	84	78±20	90	140±29	507±26	377±21	221±13
12.1	74	27±20	81	133±35	395±33	394±30	173±21
12.3		7±10	78	125±40	384±35	393±34	187±23
12.9		17±10	61	98±30	325±26	416±25	132±20
13.2		11±8		56±40	204±36	286±36	108±29
13.9		23±10		84±30	171±30	220±29	63±20

<sup>a</sup> From Ref. 9.

One observes that their measurements on Ta and ours generally agree. In the case of Au, the two  $(p,n)$  measurements are, in some cases, more widely separated. This greater difference may be attributed to the difficulty of making accurate cross-section measurements on this element whose decay scheme is rather complex.

In Table III we show the  $(p,pn)$  excitation function for Ag that was derived by subtracting the results of Wing and Huizenga<sup>10</sup> from those obtained in this experiment. They measured the  $(p,n)$  excitation functions of the two separated isotopes. The tabulated values are the weighted averages of their results. In an experiment in which they measured the  $(p,pn)$  excitation function of Mg<sup>107</sup>, Cohen *et al.*,<sup>11</sup> found that the cross section is less than 5 mb below 14 MeV. This implies that the derived excitation function shown in Table III is due to Ag<sup>109</sup> and, in fact, that the values are to be multiplied by a factor of 2. That the  $(p,pn)$  excitation function for Ag<sup>109</sup> rises as rapidly as these results would indicate is somewhat doubtful. Moreover, the  $(p,pn)$  excitation

TABLE II. Tabulation of observed  $(p,2n)$  cross sections.

Energy (MeV)	Ta <sup>a</sup>	Ta	Au <sup>a</sup>	Cross section (mb)			
				Au	Ag	Pb	Pt
7.6							
8.1							
8.5							
9.0		23±8			13±8		
9.7		85±9		31±10	44±8		8±4
10.0	148±27	144±18	73±13	56±15	103±16		21±9
10.6		246±16		129±15	156±12		64±6
11.1	404±54	332±30	150±27	189±34	300±19		110±13
11.5		422±24		262±19	340±20	31±9	199±10
12.1	460±83	565±34		397±31	474±29	118±16	344±18
12.3		582±35		398±34	486±30	124±17	340±20
12.9		661±34		523±27	578±31	290±18	504±22
13.2		770±45		637±42	762±41	427±27	583±27
13.9		806±43		791±50	790±40	577±29	678±28

<sup>a</sup> Reference 9.

<sup>9</sup> L. Hansen, R. Jopson, H. Mark, and C. Swift, Nucl. Phys. **30**, 389 (1962).

<sup>10</sup> J. Wing and J. R. Huizenga, Phys. Rev. **128**, 280 (1962).

<sup>11</sup> B. L. Cohen, E. Newman, R. A. Charpie, and T. H. Handley, Phys. Rev. **94**, 620 (1954).

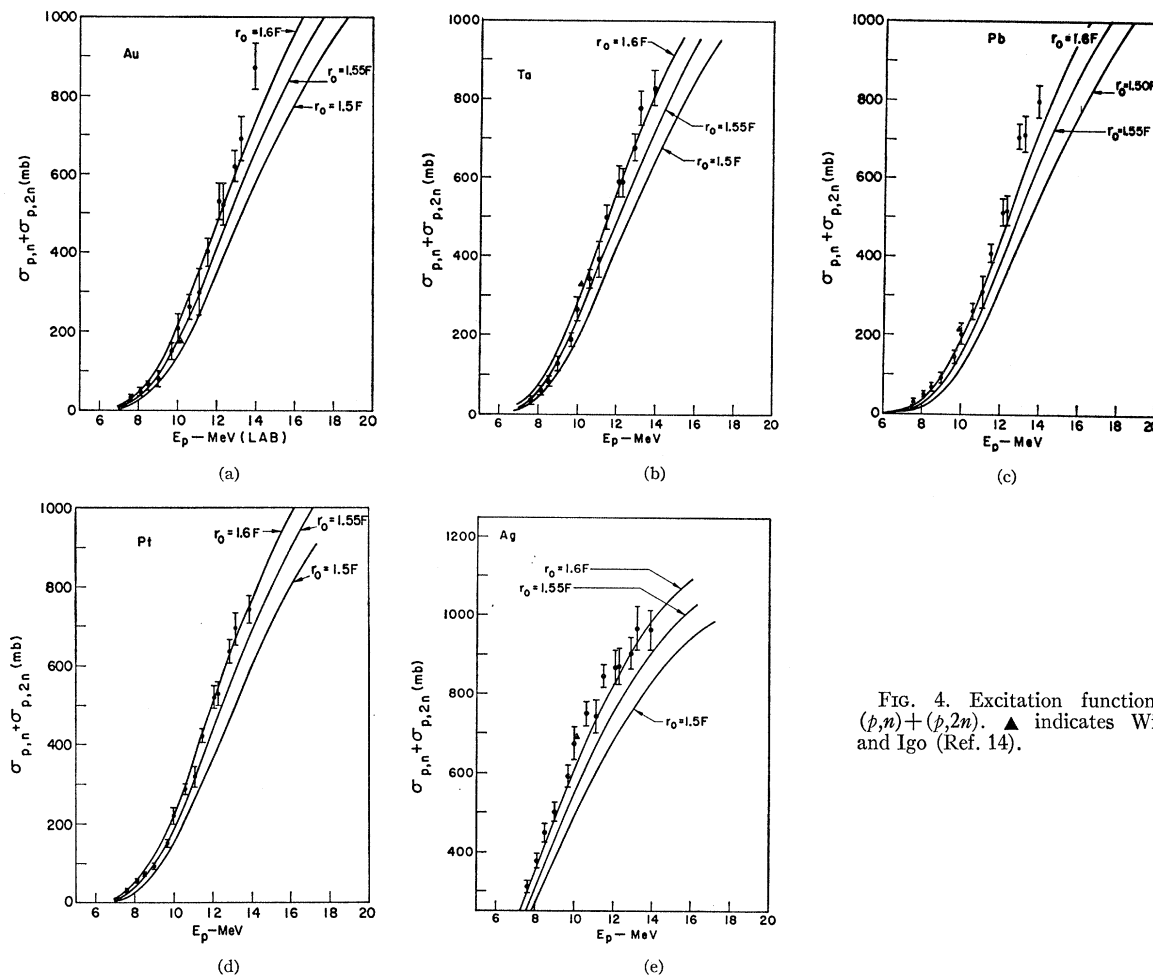


FIG. 4. Excitation function for  $(p,n) + (p,2n)$ .  $\blacktriangle$  indicates Wilkins and Igo (Ref. 14).

function in Table III does not agree with the results of Meyer *et al.*<sup>12</sup> who quote 30.7 mb as the total charged-particle cross section of Ag at 9.85 MeV. This value, which can be taken as the upper limit of the  $(p,pn)$  cross section of Ag at this energy, is considerably smaller than the value of 115 mb as derived here.

In the case of Pb, reference is made to the work of Bell and Skarsgard<sup>13</sup> who determined the  $(p,2n)$  cross sections for  $Pb^{206}$ ,  $Pb^{207}$ , and  $Pb^{208}$  between 12 and 85 MeV. Their measurements on  $Pb^{206}$  at 12.7 MeV are

TABLE III. Excitation function for  $(p,pn)$  in Ag.

Energy (MeV)	$\sigma(p,n) + \sigma(p,\gamma n)^a$ (mb)	$\sigma(p,n) + \sigma(p,pn) + \sigma(p,\gamma n)$ (mb)	$\sigma(p,pn)$ (mb)
8.0	288	379	91
8.7	354	465	111
9.0	397	489	92
9.8	434	549	115
10.0	428	573	145
10.6	446	595	159

<sup>a</sup> From Ref. 10.

<sup>12</sup> V. Meyer and N. Hintz, Phys. Rev. Letters **5**, 207 (1960).

<sup>13</sup> R. E. Bell and H. M. Skarsgard, Can. J. Phys. **34**, 745 (1956).

the only numbers they derived that can be compared with ours. They found a value of 230 mb for the  $(p,n)$  cross section. This is considerably smaller than the value of  $\sim 400$  mb reported here (Table I) for the mixture of isotopes, and one wonders whether this difference is in part due to  $(p,pn)$  interactions.

Figure 4 shows the sum  $(\bar{\sigma}_n + \bar{\sigma}_{2n})$  for each element. Because of the Coulomb barrier which inhibits charged-particle emission, this sum should be a good measure of the total absorption cross section for these elements. Also shown are the 10-MeV nonelastic cross sections obtained by Wilkins and Igo<sup>14</sup> for Ta, Ag, Au, and Pb. Since compound elastic scattering is generally assumed small, the nonelastic cross sections and the sum  $(\bar{\sigma}_n + \bar{\sigma}_{2n})$  are expected to be approximately equal. The errors quoted by these authors exceed 50% in all cases except for Ag where they are 10%. It is seen, however, that their measured values are in good agreement with ours. On the basis of these results, one confirms that neutron production processes represent the dominant modes of compound-nucleus decay near 10 MeV for

<sup>14</sup> B. Wilkins and G. Igo, Phys. Rev. **129**, 2198 (1963).

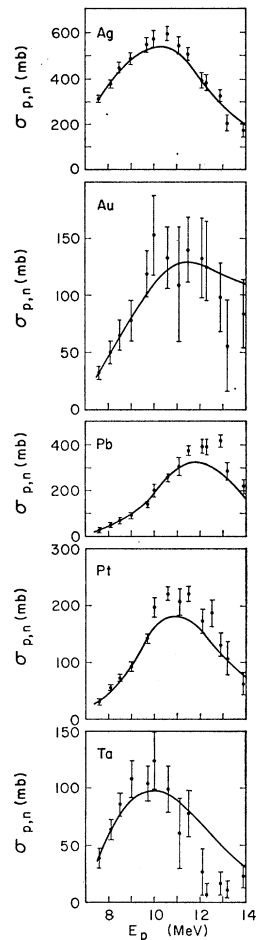


FIG. 5. Excitation function for the  $(p,n)$  interaction.

these elements. This agreement also allows us to compare our results with theory. The curves shown in the figures are the result. They were drawn from data supplied by Shapiro,<sup>15</sup> and represent the averages over the isotopes of each element. It is seen that a value of the nuclear radius parameter  $r_0$  of 1.6 F gives a reasonably good fit to the experimental data, where  $R = 1.6 \times 10^{-13} A^{1/3}$  cm, and  $A$  is the mass number of the isotope. This value is the same as that found by Hansen and Albert<sup>16</sup> for some of the isotopes that they studied. It also represents the average from the results of Blosser and Handley<sup>17</sup> who quote a value of 1.55 to 1.65 F. A few researchers, however, have found lower values for this important quantity. In the work of Andre *et al.*,<sup>18</sup> a value of 1.5 F was found. This lower value could be due to  $(p,pn)$  which they did not measure. Bell and Skarsgard<sup>13</sup> determined  $r_0 = 1.3$  F from data that showed considerable fluctuation over the energy range studied. An interesting argument for relatively

large  $r_0$  ( $>1.7$  F) is given by Blosser and Handley.<sup>17</sup> On the basis of some rather large cross sections that have been observed,<sup>19,20</sup> these authors suggest the possibility that the total cross sections are rising toward a limit that is the same for all isotopes. Relatively small values of  $(p,n)$  and  $(p,2n)$ , which lead to small values of  $r_0$  when considered alone, would then imply substantial competition from other processes.

### EXCITATION FUNCTIONS

If the  $(p,pn)$  interaction contributes significantly to the results shown in Table I, one might hope to see evidence of this by comparing the data with predictions from statistical theory. The experimentally observed  $(p,n)$  and  $(p,2n)$  cross sections are plotted in Figs. 5 and 6, respectively. The curves are the corresponding predictions as given by statistical theory,<sup>21</sup> and were

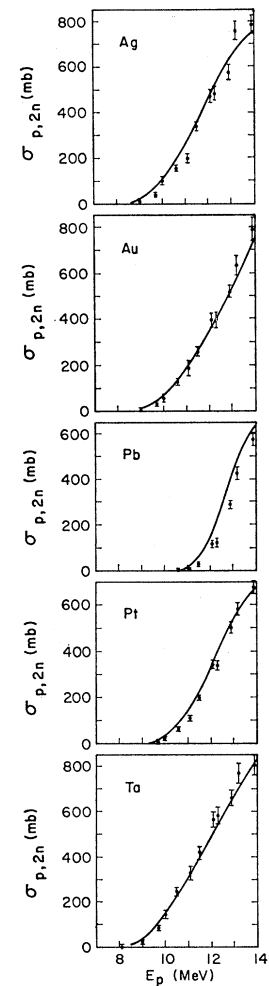


FIG. 6. Excitation function for the  $(p,2n)$  interaction.

<sup>15</sup> M. M. Shapiro, Phys. Rev. **90**, 171 (1953).

<sup>16</sup> Luisa F. Hansen and Richard D. Albert, Phys. Rev. **128**, 291 (1962).

<sup>17</sup> H. G. Blosser and T. H. Handley, Phys. Rev. **100**, 1349 (1955).

<sup>18</sup> C. G. Andre, J. R. Huizenga, J. F. Meca, W. J. Ramler, E. G. Rauh, and S. R. Rocklin, Phys. Rev. **101**, 645 (1956).

<sup>19</sup> B. L. Cohen and E. Newman, Phys. Rev. **99**, 718 (1955).

<sup>20</sup> J. P. Blaser, F. Boehm, P. Marmier, and P. Scherer, Helv. Phys. Acta **24**, 441 (1951).

<sup>21</sup> J. M. Blatt and V. F. Weisskopf, *Theoretical Nuclear Physics* (John Wiley & Sons, Inc., New York, 1952), Chap. 8.

obtained under the assumption that only neutrons result from the decay of the compound nuclei under consideration. This assumption is frequently made for heavy nuclei.

The equations for the curves are

$$\bar{\sigma}_n = \langle \sigma_c (1 + E_c/\theta) e^{-E_c/\theta} \rangle_{av} \quad (6a)$$

$$\simeq \bar{\sigma}_c \langle (1 + E_c/\theta) e^{-E_c/\theta} \rangle_{av}, \quad (6b)$$

and

$$\bar{\sigma}_{2n} = \langle \sigma_c [1 - (1 + E_c/\theta)] e^{-E_c/\theta} \rangle_{av} \quad (7a)$$

$$\simeq \bar{\sigma}_c [1 - (1 + E_c/\theta)] e^{-E_c/\theta} \rangle_{av}. \quad (7b)$$

In Eqs. (6) and (7),  $E_c$  is the excess energy over the  $(p, 2n)$  threshold, and  $\theta$  is the characteristic temperature of the Maxwell distribution, given by  $\theta = (E_m/a)^2$ . The energy  $E_m$  is the maximum available in the  $(p, n)$  process that immediately precedes the release of the second neutron. The nuclear level density parameter  $a$  for a nucleus of mass number  $A$  was assumed to be represented by  $a = A/20$ . The value of  $1/20$  for the proportionality constant was taken as a compromise between published values varying between  $1/10$  and  $1/30$ . Grover and Nagle<sup>22</sup> quote  $11 \text{ MeV}^{-1}$  for the level density parameter from measurements on isotopes of lead and bismuth. Using the same level density function as Grover and Nagle, Hansen and Albert<sup>16</sup> found values between  $A/20$  and  $A/30$ . Using a level density function that did not contain pairing energy, Bramblett and Bonner<sup>23</sup> found  $a = A/10$  agreed with their data, and  $a = A/15$  provided best agreement when the pairing energy was taken into account. In a measurement of neutron spectra, Albert *et al.*<sup>24</sup> found that the level density parameter was best expressed by  $a = A/13$  when pairing energy was not considered, and by  $a = A/20$  to  $a = A/30$  when the pairing energy was included. These

and other experiments<sup>25-27</sup> have thus produced conflicting results regarding the relationship between the level density parameters and the mass number. The quantity  $\sigma_c$  in the above formulas, which represents the cross section for formation of the compound nucleus, was taken as the experimentally observed  $\bar{\sigma}_n + \bar{\sigma}_{2n}$ .

In the equations we have equated the average over the various isotopes of an element, which is represented by the first of each pair, with the approximate result obtained by separating the two factors and averaging over each. This was done after comparing the fits obtained for the mono-isotopic elements Au and Ta with those obtained for the other elements studied. Reference to the graphs shows that there are no discernible differences that one might attribute to this procedure. It is seen that the curves agree reasonably well with the experimental data. Only in the case of Pb do the predicted  $(p, 2n)$  cross sections appear to be slightly overestimated, and correspondingly the  $(p, n)$  cross sections underestimated. The differences appear too small, however, to consider this as evidence of the  $(p, pn)$  interaction in this element. Moreover, the uncertainty in the value of the level density parameter, together with the similarity in the behavior of the curves for the mono-isotopic and non-mono-isotopic elements, render their value in this regard somewhat doubtful.

#### ACKNOWLEDGMENTS

The authors wish to thank all who played a part in the success of this experiment. Particularly, we gratefully acknowledge the contributions of Curt Sewell, who designed the electronics; David Moyer, who set up the beam sweeper system; George Clough and Virgil Gregory, who modified the tank; Robert Dickinson, who programmed the analysis for the CDC 3600 computer, and Donald Rawles and crew for operation of the 90-in. cyclotron.

<sup>22</sup> J. Robb Grover and Richard J. Nagle, Phys. Rev. **134**, B1248 (1964).

<sup>23</sup> R. L. Bramblett and T. W. Bonner, Nucl. Phys. **20**, 395 (1960).

<sup>24</sup> R. D. Albert, J. D. Anderson, and C. Wong, Phys. Rev. **120**, 2149 (1960).

<sup>25</sup> V. A. Sidorov, Nucl. Phys. **35**, 253 (1962).

<sup>26</sup> C. H. Holbrow and H. H. Barschall, Nucl. Phys. **42**, 264 (1963).

<sup>27</sup> T. D. Thomas, Nucl. Phys. **53**, 558 (1964).